Chapter 4

New Charged Anisotropic Solution on Paraboloidal Spacetime

New exact solutions of Einstein's field equations for charged stellar models by assuming linear equation of state $p_r = A(\rho - \rho_a)$, where p_r is the radial pressure, ρ_a is the surface density and A is a constant. Assuming ansatz $e^{\lambda} = 1 + \frac{r^2}{R^2}$, the physical acceptability conditions of the model are investigated and the model is compatible with several compact star candidates like 4U 1820-30, EXO 1785-248, LMC X-4. A noteworthy feature of the model is that it satisfies all the conditions needed for a physically acceptable model.

4.1 Introduction

Einstein's field equations are a system of highly non-linear partial differential second-order equations. They are essential for modelling relativistic compact objects such as dark energy stars, gravastars, quark stars, and neutron stars. The pressure distribution in the star may not be isotropic when the matter distributions have a high density in the nuclear regime, has been presented by Ruderman [168] and Canuto

[31]. Bowers and Liang [28] discussed the different causes for anisotropy. Since then, many researchers have studied the anisotropy Dev and Gleiser [47], Dev and Gleiser [48], Gleiser and Dev [63], Gokhroo and Mehra [64], Patel and Mehta [154], Thomas and Ratanpal ([197], [203], [204], [205]) to name a few. The effect of anisotropy has been studied by Ivanov [81]. A large number of researchers worked on Einstein's field equations, making different assumptions in the physical content as well as spacetime metric viz., Sharma and Ratanpal [179], Murad and Fatema [115], Murad and Fatema [116], Murad and Fatema [117], Thomas and Pandya [199], Thomas and Pandya [198], Ratanpal *et. al.* [158].

To construct relativistic compact star models, researchers used generic barotropic equations of state, in which pressure and density have linear, quadratic, or polytropic relationships in several modern literary works. Sharma and Maharaj [178] used linear equation of state to establish relativistic compact models consistent with observational data. Physically viable relativistic compact stars models studied by Ngubelanga and Maharaj [139] for a linear equation of state in isotropic coordinates. Solutions of anisotropic distributions admitting a quadratic equation of state were studied by Feroze and Siddiqui [56] and Takisa and Maharaj [183]. Thirukkanesh and Ragel [190] and Takisa and Maharaj [184] have implemented polytropic equation of state to generate models of relativistic stars. Knutsen [95] gave the conditions for models to be physically viable. It has been observed that if the tangential pressure (denoted by $p_\perp$) is higher than the radial pressure (represented by p_r), the stellar system becomes potentially stable. Sharma and Maharaj [178] studied the linear equation of state for relativistic stars by choosing $e^\lambda = \frac{1+ar^2}{1+(a-b)r^2}$ in the spacetime metric as the coefficient of dr^2 and got the various result for different values of a and b. Thirukkanesh and Maharaj [189] have studied charged anisotropic matter with a linear equation of state by specifying a particular form for one of the gravitational potentials and the electric field intensity. Ivanov [84] has studied generating solutions

for linear and Ricatti equations in general relativity. The anisotropic analogue for the work of Durgapal and Fuloria [53] was studied by Maurya *et. al.* [101]. Maurya *et. al.* [108] presented a comprehensive study on relativistic solutions describing spherically symmetric and static anisotropic stars in hydrostatic equilibrium. A compact spherically symmetric relativistic body with anisotropic particle pressure profiles was investigated by Maurya *et. al.* [109]. Maurya *et. al.* [110] investigated a new family of exact solutions to the Einstein system of equations with an anisotropic fluid distribution for a spherically symmetric spacetime using a conformal killing vector and Lia dragged metric tensor g_{ab}. Maurya *et. al.* [111] examined the impact of pressure anisotropy on Buchdahl-type relativistic compact stars. Geng *et. al.* [62] indicated that the fascinating recurrent fast radio bursts (FRBs) are produced by intermittent fractional collapses of a strange star crust caused by accretion material replenishment from its low-mass companion.

Felice *et. al.* [59] and Ray *et. al.* [164] suggested the models generated, which have been used in describing neutron stars and black hole formation. Several models of charged relativistic matter have been studied by researchers, Komathiraj and Maharaj [88], Thirukkanesh and Maharaj [189]. Bare quark stars were considered by Usov *et. al.* [210], hybrid proto-neutron stars were studied by Nicotra *et. al.* [142] and strange quark star matter was considered by Dicus *et. al.* [50]. In static spherically symmetric spacetimes, the existence of a conformal killing vector for anisotropic relativistic charged matter has been assumed by Esculpi and Aloma [54]. Mak and Harko [119] have found exact solutions for strange quark matter. Felice *et. al.* [59] studied a particular solution relating the radial pressure to the energy density with a quadratic equation of state. Malaver [131] represented a relativistic model with the quadratic equation of state with a charged distribution. Malaver and Kasmaei [132] studied the strange quark star model with the quadratic equation of state. Sunzu *et. al.* [181] describe matter distribution that satisfies a

linear equation of state consistent with quark matter. Maharaj *et. al.* [128] derived some simple models for quark stars by considering the charged anisotropic matter with a linear equation of state.

4.2 The Spacetime Metric

A three-paraboloid immersed in a four-dimensional Euclidean space has the cartesian equation

$$x^2 + y^2 + z^2 = 2wR, \tag{4.1}$$

where w = constants gives a spheres, while x = constants, y = constants, and z = constants respectively, give 3- paraboloids. The equation (4.1) can be parametrize as

$$x = rsin\theta cos\phi,$$

$$y = rsin\theta sin\phi,$$

$$z = rcos\theta,$$

$$w = \frac{r^2}{2R}, \tag{4.2}$$

substituting parametrization (4.2) in Euclidean metric

$$d\sigma^2 = dx^2 + dy^2 + dz^2 + dw^2. \tag{4.3}$$

we get

$$d\sigma^2 = \left(1 + \frac{r^2}{R^2}\right) dr^2 - r^2(d\theta^2 + sin^2\theta d\phi^2) \tag{4.4}$$

and we take the interior spacetime metric as

$$ds^2 = e^{\nu}dt^2 - \left(1 + \frac{r^2}{R^2}\right)dr^2 - r^2(d\theta^2 + sin^2\theta d\phi^2), \tag{4.5}$$

where R is the curvature parameter. We take the energy-momentum tensor for an anisotropic-charged fluid sphere of the form

$$T_{ij} = diag\left(\rho + E^2, p_r - E^2, p_\perp + E^2, p_\perp + E^2\right), \tag{4.6}$$

where ρ is the matter density, p_r is the radial pressure, $p_\perp$ is the tangential pressure and E is the electric field intensity. On spacetime metric (4.5) with energy-momentum technique (4.6) the Einstein's field equations, takes the form

$$8\pi\rho + E^2 = \frac{1 - e^{-\lambda}}{r^2} + \frac{e^{-\lambda}\lambda'}{r}, \tag{4.7}$$

$$8\pi p_r - E^2 = \frac{e^{-\lambda}\nu'}{r} + \frac{e^{-\lambda} - 1}{r^2}, \tag{4.8}$$

$$8\pi p_\perp + E^2 = e^{-\lambda}\left(\frac{\nu''}{2} + \frac{\nu^2}{4} - \frac{\nu'\lambda'}{4} + \frac{\nu' - \lambda'}{2r}\right), \tag{4.9}$$

$$8\pi\sqrt{3}S = 8\pi p_r - 8\pi p_\perp, \tag{4.10}$$

where primes denote differentiation concerning r. The system of equation (4.7-4.9) governs the behaviour of the gravitational field for an anisotropic charged fluid distribution. choosing

$$E^2 = \frac{\alpha\frac{r^2}{R^2}}{R^2(1 + \frac{r^2}{R^2})^2}, \tag{4.11}$$

where $0 \leq \alpha \leq 1$. By substituting the value of e^{λ} and E^2 in the equation (4.7), we get

$$8\pi\rho = \frac{3 + (1 - \alpha)\frac{r^2}{R^2}}{R^2(1 + \frac{r^2}{R^2})^2}. \tag{4.12}$$

The expression for density $\rho(r)$ is finite at the centre of the star.

4.3 Linear Equation of State

We anticipate that the matter distribution should meet a barotropic equation of state for a physically plausible relativistic star $p_r = p_r(\rho)$. Many researchers have presented their ideas on the linear equation of state, Thirukkanesh and Maharaj [189], Thomas and Pandya [200]. We consider a linear equation of state between the radial pressure p_r and matter density ρ as

$$p_r = A\rho - B, \tag{4.13}$$

where A and B are constants. At the boundary $r = a$ of the star

$$p_r(r = a) = 0,$$

this gives,

$$B = A\rho_a, \tag{4.14}$$

where ρ_a represents the surface density. We substitute equation (4.14) in (4.13) and get

$$p_r = A\rho - A\rho_a = A(\rho - \rho_a), \tag{4.15}$$

substituting equations (4.11) and (4.15) in (4.8)

$$\nu' = re^{\lambda}\left[A(\rho - \rho a) - \left(\frac{e^{-\lambda} - 1}{r^2}\right) - E^2\right],$$

using the expression of density given in (4.12) we get

$$\nu' = r\left(1+\frac{r^2}{R^2}\right)\left(\frac{1}{R^2(1+\frac{r^2}{R^2})}+A\left(\frac{(-3+\frac{a^2}{R^2}(\alpha-1))-\frac{r^2}{R^2}\alpha}{R^2(1+\frac{r^2}{R^2})^2}+\frac{3-\frac{r^2}{R^2}(1-\alpha)}{R^6(1+\frac{r^2}{R^2})^2}\right)\right), \tag{4.16}$$

integrating (4.16), we get

$$e^{\nu} = CR^{2A+3\alpha}\left(1+\frac{r^2}{R^2}\right)^{\left(\frac{\alpha+A(2+\alpha)}{2}\right)}$$

$$\times exp\left[(A+1)(1-\alpha)\frac{r^2}{2R^2}-\frac{A}{2}\left(\left(3+(1-\alpha)\frac{a^2}{R^2}\right)\left(1+\frac{r^2}{2R^2}\right)\left(1+\frac{a^2}{R^2}\right)^{-2}\frac{r^2}{R^2}\right)\right], \tag{4.17}$$

where C is a constant of integration. Substituting $\alpha = 0$ in the expression of (4.3), we get the solution given by Thomas and Pandya [200].

4.4 Matching Condition

The spacetime metric (4.5) together with (4.3) should continuously match with the Reissner-Nordström exterior spacetime metric across the boundary $r = a$ of the star

$$ds^2 = \left(1-\frac{2M}{r}+\frac{Q^2}{r^2}\right)dt^2-\left(1-\frac{2M}{r}+\frac{Q^2}{r^2}\right)^{-1}dr^2-r^2(d\theta^2+sin^2\theta d\phi^2). \tag{4.18}$$

This leads to

$$M = \frac{\frac{a^3}{R^2}\left(1+(1+\alpha)\frac{a^2}{R^2}\right)}{2(1+\frac{a^2}{R^2})^2}, \tag{4.19}$$

$$C = \frac{1}{R^{A\alpha+\alpha+2A}(1+\frac{a^2}{R^2})^{\frac{(A+1)(2+\alpha)}{2}}}\times F, \tag{4.20}$$

where,

$$F = exp\left(\frac{1}{4}\left(A + 2A\alpha + 2\alpha - 2 + (A\alpha - A + 2\alpha - 2)\frac{a^2}{R^2}\right)\right).$$

The expression of matter density, radial pressure, and tangential pressure takes the form

$$8\pi\rho = \frac{3 + (1-\alpha)\frac{r^2}{R^2}}{R^2(1+\frac{r^2}{R^2})^2}, \tag{4.21}$$

$$p_r = A\rho - A\rho_a = A(\rho - \rho_a), \tag{4.22}$$

$$8\pi p_\perp = \frac{-\frac{r^2}{R^2}\alpha}{R^2(1+\frac{r^2}{R^2})^2} + \frac{A_1 + A_2 + A_3 + r^2(A_4)^2}{4(1+\frac{r^2}{R^2})}. \tag{4.23}$$

Where

$$A_1 = \frac{-18A\frac{r^2}{R^2} - 12A + 4A(\alpha-1)\frac{a^2}{R^2} + 6A(\alpha-1)\frac{a^2}{R^2}\frac{r^2}{R^2}}{R^2(1+\frac{a^2}{R^2})^2},$$

$$A_2 = \frac{4\alpha + 4A(2+\alpha) - 4 + 2(1+A)(\alpha+1)\frac{r^2}{R^2}}{R^4(1+\frac{r^2}{R^2})^2},$$

$$A_3 = \frac{-6\alpha\frac{r^2}{R^2} - 6A(2+\alpha)\frac{r^2}{R^2}}{R^2(1+\frac{r^2}{R^2})^2} - \frac{4(1+A)(\alpha-1)}{R^2},$$

$$A_4 = \frac{A(1+\frac{r^2}{R^2})^2(-3+(\alpha-1)\frac{a^2}{R^2})}{R^2(1+\frac{a^2}{R^2})^2} - \frac{(1+A)(\alpha-1)}{R^2} + \frac{2A+3\alpha}{R^2(1+\frac{r^2}{R^2})}.$$

In the next section, we will observe the behaviour of density, radial pressure, tangential pressure, and other physically viable conditions.

4.5 Physical Plausibility Condition and Bound on α

A physically acceptable stellar model should comply with the following conditions throughout its region of validity.

(i) $\quad \rho(r) \geq 0, \quad p_r(r) \geq 0, \quad p_\perp(r) \geq 0, \qquad \text{for } 0 \leq r \leq R$

(ii) $\quad \frac{d\rho}{dr} \leq 0, \quad \frac{dp_r}{dr} \leq 0, \quad \frac{dp_\perp}{dr} \leq 0, \qquad \text{for } 0 \leq r \leq R$

(iii) $\quad 0 \leq \frac{dp_r}{d\rho} \leq 1\ , \quad 0 \leq \frac{dp_\perp}{d\rho} \leq 1, \quad \text{for } 0 \leq r \leq R$

(iv) $\quad \rho - p_r - 2p_\perp \geq 0, \qquad \text{for } 0 \leq r \leq R$

(v) $\quad \Gamma > \frac{4}{3}, \qquad \text{for } 0 \leq r \leq R$

We have demonstrated, via a graphical method, the fulfillment of all stated conditions. The expression of density is

$$8\pi\rho = \frac{3 + (1-\alpha)\frac{r^2}{R^2}}{R^2(1+\frac{r^2}{R^2})^2},$$

it can be noticed that the condition ($\rho_{r=0} > 0$ and $\rho_{r=a} > 0$) are satisfies if

$$0 \leq \alpha \leq 1. \tag{4.24}$$

The value of radial pressure p_r should be equal to zero at the surface of the star $r = a$. From equations (4.22) and (4.23), it is observed that the conditions $p_r(r = 0) \geq 0$, $p_\perp(r = 0) \geq 0$ and $p_\perp(r = R) \geq 0$ impose a bound on α, viz.,

$$0 \leq \alpha \leq 0.251789 \tag{4.25}$$

4.5.1 Energy Condition

The strong energy conditions $\rho - p_r - 2p_\perp \geq 0$ at the centre $r = 0$ and at surface of the star $r = a$, restricts the value of α viz.,

$$0 \leq \alpha \leq 0.3215. \tag{4.26}$$

The value of strong energy conditions is described in Table (4.1)

Table 4.1: Values of strong energy condition at centre as well as surface for $\alpha = 0.1$

STAR	**M** ($\mathbf{M_\odot}$)	**a** (**Km**)	**R** (**Km**)	$\rho - \mathbf{p_r} - \mathbf{2p}_{\perp(r=0)}$ (**MeV fm^{-3}**)	$\rho - \mathbf{p_r} - \mathbf{2p}_{\perp(r=a)}$ (**MeV fm^{-3}**)
4U 1820-30	1.58	9.1	9.31	834.813	279.409
PSR J1903+327	1.66	9.438	9.54	793.228	258.666
EXO 1785-248	1.3	8.849	10.48	677.869	297.572
LMC X-4	1.04	8.301	11.14	614.904	322.681
SMC X-4	1.29	8.831	10.51	674.657	298.486
Cen X-3	1.49	9.178	9.98	735.062	278.061

4.5.2 Causality and Stability Conditions

(i) Causality condition:

The values of square of sound of the radial speed $\frac{dp_r}{d\rho}$ and the square of sound of tangential speed $\frac{dp_\perp}{d\rho}$ at $r = 0$ and $r = a$ for different stars have been calculated in Table 4.4. These velocities are in the range of 0 and 1. The bounds on α for $0 \leq \frac{dp_r}{d\rho} \leq 1$, $0 \leq \frac{dp_\perp}{d\rho} \leq 1$ are

$$0 \leq \alpha \leq 2.28165, \tag{4.27}$$

$$0 \leq \alpha \leq 1.11724. \tag{4.28}$$

(ii) Relativistic adiabatic index:

According to Chan *et. al.* [32], the collapsing condition for the classical, relativistic case

$$\Gamma \leq \frac{4}{3} + \left[\frac{1}{3}k\frac{\rho_0 p_{r_0}}{|p'_{r_0}|} + \frac{4}{3}\frac{p_{\perp_0} - p_{r_0}}{|p'_{r_0}|r}\right]_{max}, \tag{4.29}$$

with $\rho_0, p_{r_0}, p_{\perp_0}$ denoting the initial density, radial and tangential pressures of the fluid at static equilibrium. The second term on the right side represents the relativistic fluid correction and the third term accounts for anisotropy. Now Heintzmann and Hillebrandt [71] demonstrated that since anisotropy effectively slows the growth of instability, increasing the anisotropic factor ($8\pi\sqrt{3} = p_r - p_\perp$) changes the stability condition as $\Gamma > \frac{4}{3}$. Moustakidis [135] proposed a more stringent condition for the critical value of the adiabatic index. The critical value of adiabatic index (Γ_{crit}) is determined by the compactness factor ($u = \frac{M}{R}$),

$$\Gamma_{crit} = \frac{4}{3} + \frac{19}{21}u, \tag{4.30}$$

for stability, it is essential to have $\Gamma \geq \Gamma_{crit}$. The following expression is used to find the adiabatic relativistic index Γ,

$$\Gamma = (\frac{\rho + p_r}{p_r})\frac{dp_r}{d\rho},$$

$\Gamma \geq \frac{4}{3}$ at $r = 0$ imposes a restriction on α as

$$0 \leq \alpha \leq 1.8686. \tag{4.31}$$

Table (4.2) shows the adiabatic index Γ at the origin and critical values of the adiabatic index.

4.5.3 Gravitational Redshift

The redshift $z = \sqrt{1/e^{\nu}} - 1$ must be a decreasing function of r and finite for $0 \leq z \leq a$. For a relativistic star, it is expected that the redshift must decrease towards the boundary and be finite throughout the distribution. The value of redshift at origin is described in Table (4.2)

4.5.4 Mass-Radius Relation

The compactness (mass-radius ratio) is the most important factor in determining the surface redshift of any charged stellar model. According to Buchdahl [30], the mass radius relation must satisfy the inequality, $\frac{M}{a} \leq \frac{4}{9}$. But when we introduce the electric field inside the matter distribution, it modifies this upper limit as proposed by Buchdahl. Later, Andréasson [3] (upper limit of $\frac{M_{ch}}{a}$) and Böhmer and Harko [27] (lower limit of $\frac{M_{ch}}{a}$) give the modified mass-radius limit in the presence of electric charge inside the matter distribution, which can be described as follows:

$$\frac{Q^2(18a^2+Q^2)}{2a^2(12a^2+Q^2)} \leq \frac{M_{ch}}{a} \leq \frac{2a^2+3Q^2+2a\sqrt{a^2+3Q^2}}{9a^2}, \tag{4.32}$$

where, M_{ch} is the total mass of the compact object for the charged perfect fluid matter distribution. The table (4.3) shows the inequality (4.32) is satisfied for various stars.

4.5.5 Stability under Three Forces Acting on the System

According to Tolman [208] and Oppenheimer and Volkof [143], the energy conservation equation of motion for our system is defined as

$$\nabla^{\mu} T_{\mu\nu} = 0.$$

We want to examine the stability of our present model under three different forces viz., gravitational force, hydrostatics force, and anisotropic force, which is described by the following equation

$$-\frac{M_G(r)(\rho+p_r)}{r^2}e^{(\lambda-\nu)/2}-\frac{dp_r}{dr}+\frac{2}{r}(p_\perp-p_r)=0, \tag{4.33}$$

known as Tolman-Oppenheimer-Volkov (TOV) equation. The quantity $M_G(r)$ represents the gravitational mass within the radius r, which can be derived from the Tolman-Whittaker formula and Einstein's field equations and is defined by

$$M_G(r)=\frac{1}{2}r^2e^{\frac{(\nu-\lambda)}{2}}\nu', \tag{4.34}$$

Adding the value of (4.34) into equation (4.33), we get,

$$\frac{-\nu'}{2}(\rho+p_r)-\frac{dp_r}{dr}+\frac{2}{r}(p_\perp-p_r)=0, \tag{4.35}$$

the above expression may also be written as

$$F_g+F_h+F_a=0, \tag{4.36}$$

$$F_g=-\frac{\nu'}{2}(\rho+p_r), \tag{4.37}$$

$$F_h=-\frac{dp_r}{dr}, \tag{4.38}$$

$$F_a=\frac{2}{r}(p_\perp-p_r), \tag{4.39}$$

the three different forces act on the system.

The figure shows that gravitational force is negative and dominating in nature which is counterbalanced by the combined effect of hydrostatics and anisotropic forces to keep the system in equilibrium. Fig. (4.11) shows these three forces in graphical

method for the star 4U 1820-30, EXO 1785-248, LMC X-4.

From the equations (4.24), (4.25), (4.26), (4.27), (4.28), and (4.31) the bound for α is $0 \leq \alpha \leq 0.251789$.

Table 4.2: Values of gravitational redshift and Adiabatic Index

STAR	**M** ($M_\odot$)	**a** (**Km**)	$\mathbf{Z_{r=0}}$ **(Gravitational) Redshift)**	$\mathbf{Z_{(r=a)}}$ **(Gravitational) Redshift)**	$\mathbf{\Gamma_{(r=0)}}$ **(Adiabatic Index)**	$\mathbf{\Gamma_{crit}}$ **(Adiabatic Index)**
4U 1820-30	1.58	9.1	0.779	0.383	1.60	1.56
PSR J1903+327	1.66	9.438	0.8010	0.3900	1.59	1.56
EXO 1785-248	1.3	8.849	0.5673	0.2985	1.80	1.52
LMC X-4	1.04	8.301	0.4351	0.2401	2.03	1.50
SMC X-4	1.29	8.831	0.5614	0.2960	1.81	1.52
Cen X-3	1.49	9.178	0.6823	0.3452	1.68	1.54

4.6 Discussion

We have studied the compatibility of the model developed using linear equation of state in the background of paraboloidal spacetime for compact stars like 4U 1820-30, EXO 1785-248, LMC X-4. Our model satisfies the elementary physical requirements for representing a superdense compact star through the graphical method. It is found that the model can accommodate the mass and radius of the compact star candidates given by Gangopadhyay *et. al.* [61]. We have displayed the graphical

Table 4.3: Values of Mass radius ratio and Buchdahl ratio.

STAR	**M** ($M_\odot$)	$\frac{\mathbf{Q^2(18a^2+Q^2)}}{\mathbf{2a^2(12a^2+Q^2)}}$ **(Lower) Limit**	$\frac{\mathbf{M_{ch}}}{\mathbf{a}}$ **(Mass Radius) Ratio**	$\frac{\mathbf{2a^2+3Q^2+2a\sqrt{a^2+3Q^2}}}{\mathbf{9a^2}}$ **(Upper Limit)**	$\mathbf{u}(=\frac{\mathbf{M}}{\mathbf{a}})$ **(Buchdahl Ratio**
4U 1820-30	1.58	0.01789	0.256	0.4602	0173
PSR J1903+327	1.66	0.0183	0.2599	0.4606	0.175
EXO 1785-248	1.3	0.0129	0.217	0.4559	0.146
LMC X-4	1.04	0.0095	0.185	0.4529	0.125
SMC X-4	1.29	0.0128	0.215	0.4557	0.146
Cen X-3	1.49	0.0157	0.2399	0.458	0.162

Table 4.4: The numerical values of the $\frac{dp_r}{d\rho}$ at centre as well as surface and $\frac{dp_\perp}{d\rho}$ at centre as well as surface.

STAR	$\left(\frac{\mathbf{dp_r}}{\mathbf{d\rho}}\right)$ **r=0**	$\left(\frac{\mathbf{dp_\perp}}{\mathbf{d\rho}}\right)$ **r=0**	$\left(\frac{\mathbf{dp_r}}{\mathbf{d\rho}}\right)$ **r=a**	$\left(\frac{\mathbf{dp_\perp}}{\mathbf{d\rho}}\right)$ **r=a**	$(\nu_\mathbf{t}^\mathbf{2} - \nu_\mathbf{r}^\mathbf{2})$ **r=0**	$(\nu_\mathbf{t}^\mathbf{2} - \nu_\mathbf{r}^\mathbf{2})$ **r=a**
4U 1820-30	0.1	0.0707	0.1	0.0567	-0.0292071	-0.043
PSR J1903+327	0.1	0.0703	0.1	0.0572	-0.0296019	-0.042
EXO 1785-248	0.1	0.0757	0.1	0.0547	-0.0313115	-0.043
LMS X-4	0.1	0.0801	0.1	0.0569	-0.0312131	-0.040
SMC X-4	0.1	0.0759	0.1	0.0547	-0.0341674	-0.032
Cen X-3	0.1	0.0728	0.1	0.0551	-0.028962	-0.048

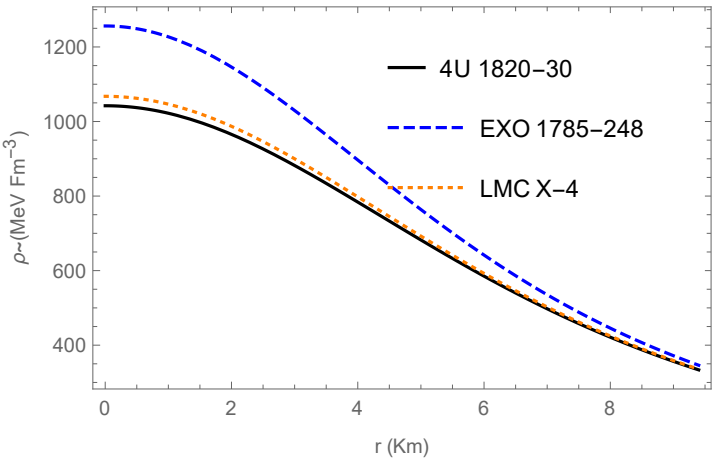

Figure 4.1: Variation of density (ρ) against the radial parameter r.

analysis only for a few compact star models here, but it can be applied to a larger class of known pulsars. In Fig. (4.1) we have shown the variation of density for the star 4U 1820-30, EXO 1785-248, LMC X-4. It is clear from the graph that the density is a decreasing function of r. In Fig.(4.2) and Fig.(4.3) we have shown the variation of radial and tangential pressure throughout the star. It can be seen that both pressures are decreasing radially outward. In Fig.(4.4) and Fig.(4.5) we have displayed the variation of $\frac{dp_r}{d\rho}$ and $\frac{dp_\perp}{d\rho}$ against r. Both quantities satisfy the restriction $0 < \frac{dp_r}{d\rho} < 1$ and $0 < \frac{dp_\perp}{d\rho} < 1$ indicating that the sound speed is less than the speed of light throughout the star.

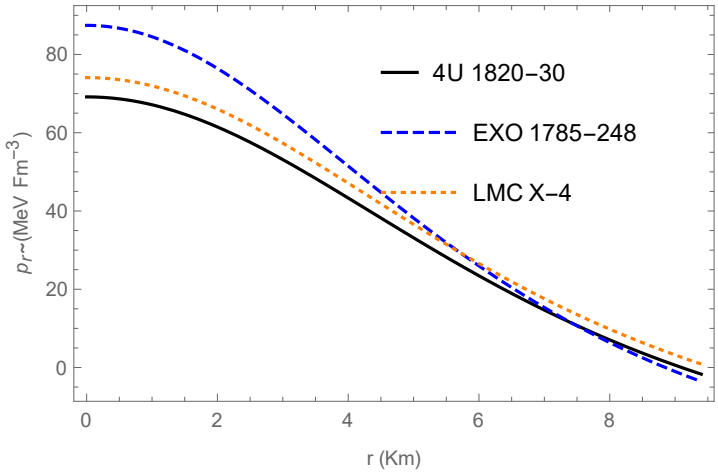

Figure 4.2: Variation of radial pressures (p_r) against the radial parameter r.

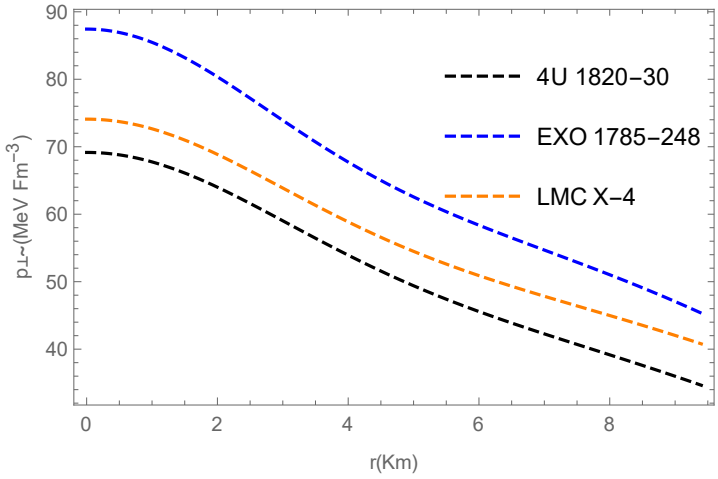

Figure 4.3: Variation of tangential pressures ($p_\perp$) against the radial parameter r.

The variation of anisotropy is shown in Fig.(4.6). It can be noticed that anisotropy vanishes at the centre and decreases towards the boundary. Fig.(4.7) indicates that the strong energy condition $\rho - p_r - 2p_\perp > 0$ is satisfied througout the distribution. For a relativistic equilibrium model of a compact star to be stable model, the adiabatic index $\Gamma = \frac{\rho+p_r}{p_r}\frac{dp_r}{d\rho} > \frac{4}{3}$ throughout the distribution. Fig.(4.8) indicates that the condition $\Gamma > \frac{4}{3}$ is satisfied for the star 4U 1820-30, EXO 1785-248, LMC X-4. For a relativistic star, it is expected that the redshift must be decreasing towards the boundary and finite throughout the distribution. Fig.(4.9) shows that gravi-

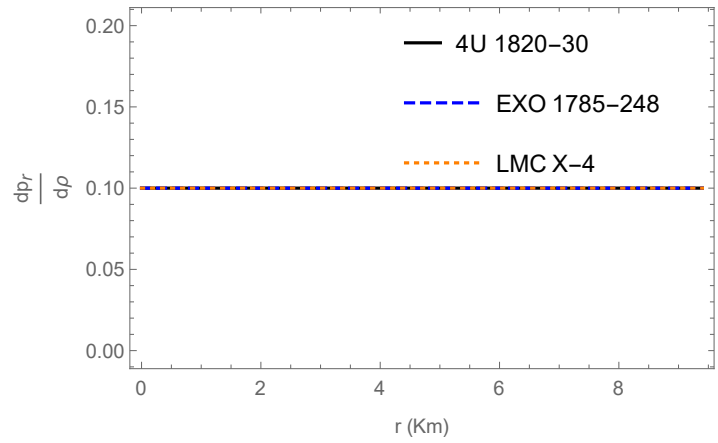

Figure 4.4: Variation of $\frac{dp_r}{d\rho}$ against the radial parameter r.

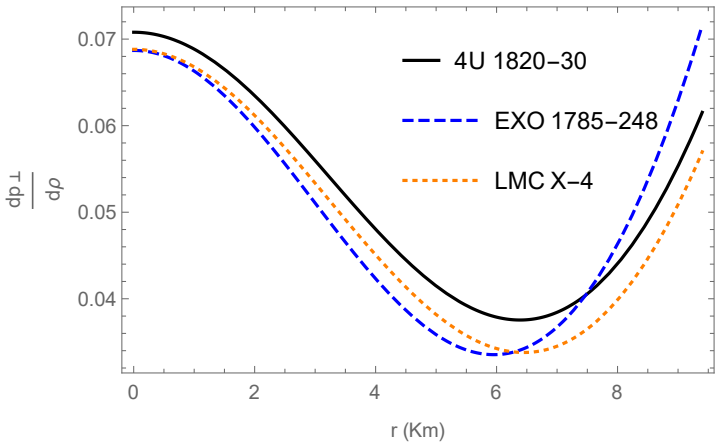

Figure 4.5: Variation of $\frac{dp_\perp}{d\rho}$ against the radial parameter r.

tational redshift is decreasing throughout the star under consideration. Fig.(4.10) shows that $\frac{dp_\perp}{d\rho} - \frac{dp_r}{d\rho}$ is negative throughout the star. Fig.(4.11) shows the graphical representation of three distinct forces for the compact star 4U1820-30. According to the graphs, the gravitational force is a net negative force that predominates in nature. Hydrostatic and anisotropic forces work together to balance this force and keep the system in equilibrium. Fig.(4.12) shows the Mass-Radius relation for the star 4U 1820-30, EXO 1785-248, LMC X-4.

It has been concluded that a large number of pulsars with known masses and radii can be accommodated in the present model, satisfying the linear equation of state.

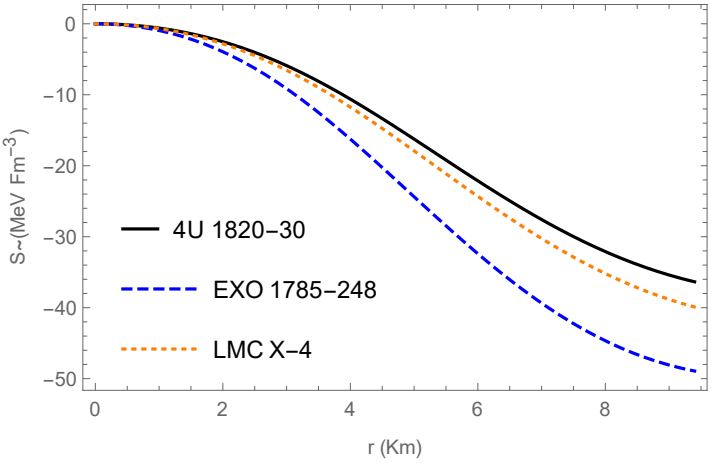

Figure 4.6: Variation of anisotropy $(p_r - p_\perp)$ against the radial parameter r.

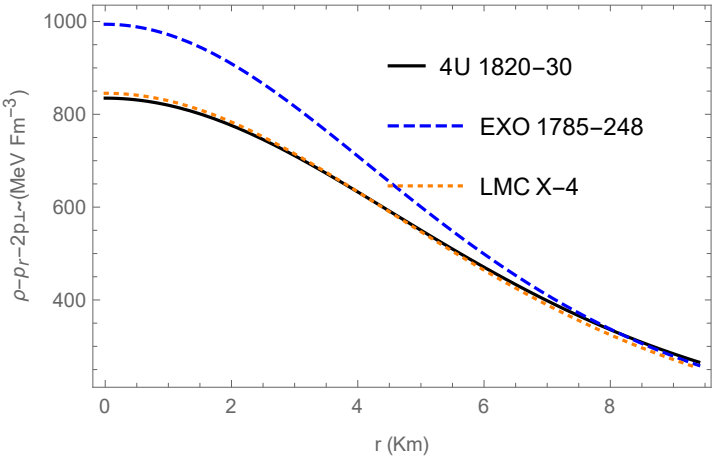

Figure 4.7: Variation of strong energy condition $(\rho - p_r - 2p_\perp)$ against the radial parameter r.

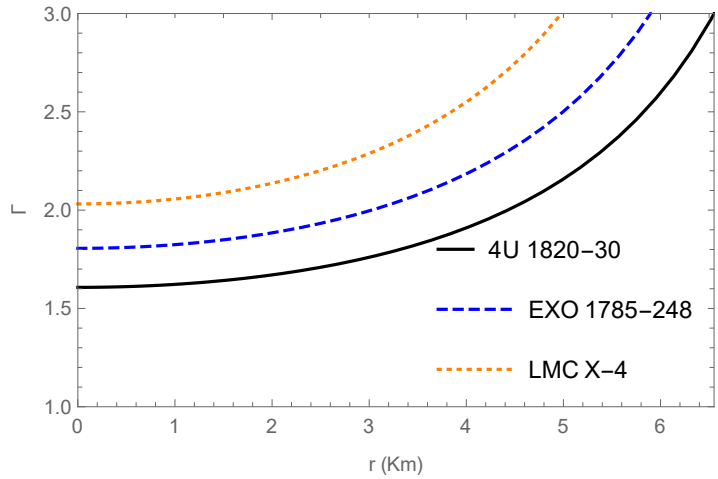

Figure 4.8: Variation of adiabatic Index against radial variable r.

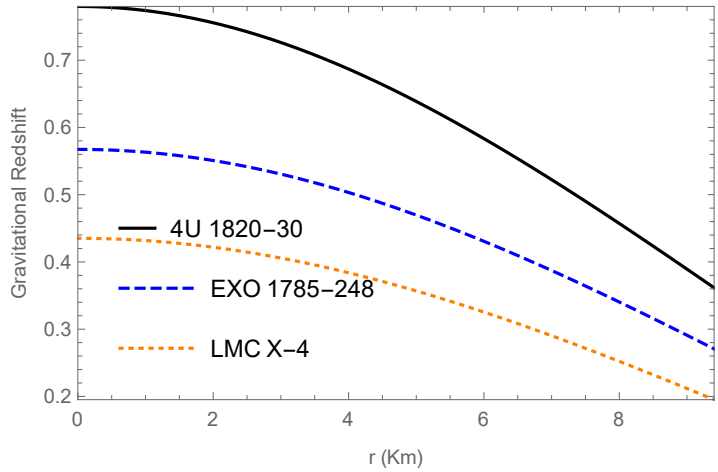

Figure 4.9: Variation of gravitational redshift against radial variable r.

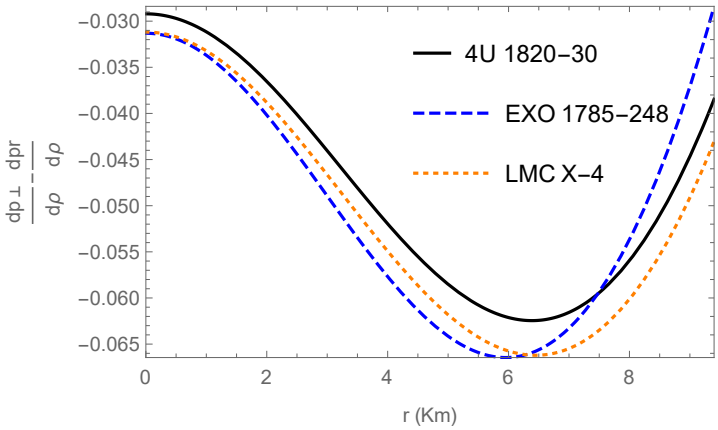

Figure 4.10: Variation of a stability expression $(\frac{dp_\perp}{d\rho} - \frac{dp_r}{d\rho})$ with respect to a radial coordinate r.

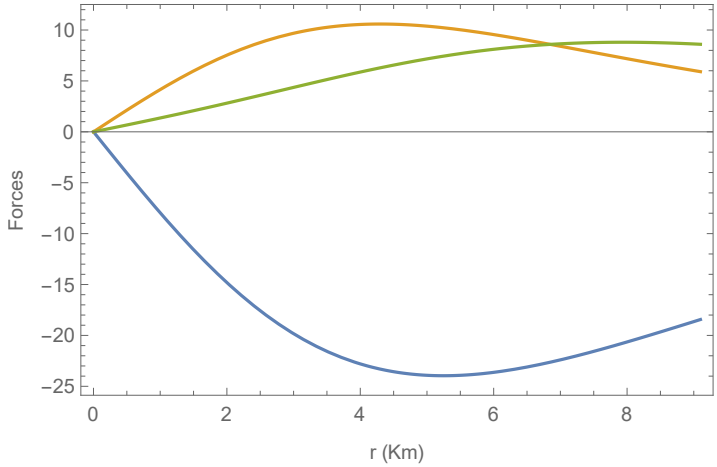

Figure 4.11: Variation of three forces like Gravitational Force(Blue), Hydrostatic Force(Orange) and Anisotropic Force(Green) for 4U1820-30 star.

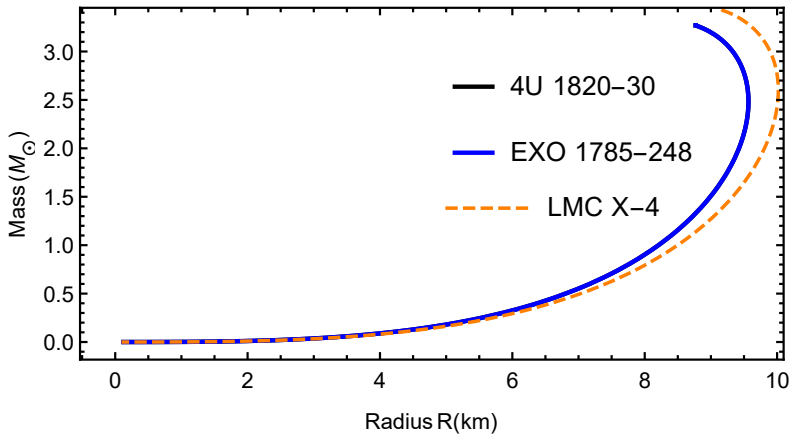

Figure 4.12: Variation of a mass M with a radius R for various stars.